International Conference on Space Optics—ICSO 2014

La Caleta, Tenerife, Canary Islands

7–10 October 2014

Edited by Zoran Sodnik, Bruno Cugny, and Nikos Karafolas

Optical performance results for the polar communication and weather mission space technology development program

Jean-François Lavigne

Louis Moreau

François Tanguay

Frédéric Girard

et al.

esa icso proceedings cnes

International Conference on Space Optics — ICSO 2014, edited by Zoran Sodnik, Nikos Karafolas, Bruno Cugny, Proc. of SPIE Vol. 10563, 105632N · © 2014 ESA and CNES
CCC code: 0277-786X/17/$18 · doi: 10.1117/12.2304125

OPTICAL PERFORMANCE RESULTS FOR THE POLAR COMMUNICATION AND WEATHER MISSION SPACE TECHNOLOGY DEVELOPMENT PROGRAM

Jean-François Lavigne[1], Louis Moreau[1], François Tanguay[1], Frédéric Girard[1], Jacques Giroux[1], Stéphane Lemelin[1], Steve Levesque[1], Simon Paradis[1], Michel Roux[1], Frédéric Grandmont[1]
[1]ABB, Remote sensing Industry, 585 Charest East, Suite 300, Qc, Québec, Canada.

I. INTRODUCTION

Current fleet of geostationary Earth orbit (GEO) satellites are used to provide communication in remote areas and to acquire meteorological data that are fed to Numerical Weather Predictions models. The third generation of GEO satellites will provide images of the Earth with a spatial resolution between 0.5 and 2.0 km every 15 minutes from 60°S to 60°N, the latitude extent being limited by the curvature of the Earth. This is a problem to ensure proper communication and weather predictions in the Canadian North that is inhabited up to a latitude of 82.5°N. Moreover, there is a lack of meteorological information in the northern latitudes that are important for the global weather models. Low-Earth Orbit (LEO) satellites can provide such data in the polar region with much better spatial resolution but on a small swath that results in up to 6 hours between measurements at a given location. The current network of LEO weather satellites does not have enough units to offer a temporal coverage comparable to the high refresh rate provided by the GEO satellites and used to determine circulation patterns and other critical information for numerical weather prediction. It would require at least 23 satellites in LEO orbit to achieve the similar refresh rate over the high latitude as the GEO satellites provide for the lower latitudes [1]. Not only that lack of data makes weather forecasting over the Arctic very difficult, but it also reduces the forecast accuracy and the ability of making long-term weather forecasts over most of North America because the weather processes at the high altitudes have an impact on the lower latitudes.

For this reasons, The Canadian Space Agency in collaboration with the Department of National Defence, Environment Canada and the support of other Government Departments completed a Phase 0 study for the Polar Communication and Weather (PCW) mission in 2008 [2]. The outcomes of the study proved that a system of two satellites in HEO with high inclination and apogees in the Northern hemisphere could provide broadband continuous communications services throughout the Arctic and improve significantly the northern latitude data coverage for weather forecasting and climate monitoring. On such orbit, each satellite will have a long duration “quasi-geostationary” dwell time over the area of interest of the PCW Mission which is all of the North above 50 degree of latitude.

In July 2009, CSA and its Government partners awarded a contract to a Canadian industrial consortium led by MDA of Richmond to conduct a twelve month Phase A Mission Analysis and Concept Definition study [3]. ABB Inc. and COMDEV Ltd. were subcontracted by MDA to define the concept of the multi-spectral imager that is the main meteorological payload for PCW. A concept that meets the user requirements was proposed.

The Phase A study also identified a series of critical technology elements that would benefit from early development. The CSA has initiated an effort to develop some of these items so that their TRL will be suitable for the program follow-on phases. An industrial team lead by ABB has been selected to perform technology development activities for the Meteorological Payload of PCW. The items selected by the CSA include the telescope assembly, the spectral filters, and the cryogenic infrared camera assemblies. The development project started in November 2011 and ended in March 2014. This paper focuses on the telescope assembly and the spectral filters elements.

II. THE PCW MULTI-SPECTRAL IMAGER

Although the exact orbit has not been fixed yet, in all the retained scenarios the PCW mission uses two satellites on a HEO with the apogee located over the high Northern latitudes. Both satellites are out of phase so that at least one satellite has always a line of sight on the Northern hemisphere. Near their apogee, the ground velocity of the satellites is very small and they can observe the Earth in conditions that are almost similar to the observation conditions from a geostationary orbit. Not surprisingly, the performance required of the Meteorological Payload of PCW are similar to next generation of multi-spectral imagers planned for GOES-R and Meteosat Third Generation (MTG) with some additional spectral bands to palliate the lack of a companion sounder and to achieve science objectives specific to Arctic region.

Up to 21 spectral bands, spread from the visible to the thermal infrared, are required. Each band is associated with one or more data products. The ground sampling distances (GSD) of the bands vary from 0.5 km to 6.0 km depending on the band number and whether the value is a goal or threshold value. Since the altitude of the satellite will vary over the course of its orbit, the GSD are specified at the altitude corresponding to the position of the satellite 1.5 hours from its apogee.

The other major characteristics of the PCW Imager are given in Table 2. They define the Field of Regard (FOR), the time allocated to acquire an image of the FOR, geo-location accuracy, and radiometric performances.

Several options were considered during the process of determining the current architecture of the PCW meteorological payload. Different ways to image the area of interest and to generate the required spectral content were considered. Finally, the concept proposed by ABB settled on a filter-based multi-spectral imager with three separate focal planes that scan the FOR with a 2-D scanning mirror.

Table 1: PCW Imager Requirements Summary [4, 5]

Parameter	Required value
Imaging period	< 15 min.
Field of Regard	100 % above 60 N 95 % 55-60 N 85 % 50-55 N
Relative geo-location uncertainty	< 0.35 GSD
Signal to noise ratio	> 300 for 0.45 µm to 2.28 µm
NEdT at 300 K	< 0.15 K for 5.77 µm to 11.6 µm < 0.35 K for 11.6 µm to 14.4 µm

All focal planes have a common input optics. The input optics is three-mirror telescope. The optical beam is split in three spectral regions by two dichroic beamsplitters and each region is sent to a different focal plane. In each focal plane, there is a certain number of optical bandpass filters disposed over the detector in the along-scan direction. As the scanning mirror moves over the scene, each portion of the focal plane array underneath a specific filter sequentially images the scene and the full spectral content is obtained after a few acquisitions. More details about the instrument concept can be found in [6].

The telescope, the filters, the dichroic beamsplitters and the multi-spectral camera assembly (MSCA) have been selected for pre-development.

III. TELESCOPE ASSEMBLY

For the telescope, the scope of the technology development includes, the design, manufacturing, and testing of a representative breadboard of the input telescope of the PCW Multi-Spectral Imager. The performances of the telescope are verified in ambient conditions and in thermal vacuum over the operating temperature range. The ability of the breadboard to endure the survival thermal environment and the launch vibrations environment are also verified by tests. At the end of the study, the design is at a TRL of 5 (testing in representative environment). The telescope is a F/3.6 Three-Mirror Anastigmat (TMA) having an entrance pupil of 230 mm. The primary and tertiary mirrors have aspherical surfaces and the secondary is a spherical convex mirror. The mirrors are made of AlSi with an electroless nickel plating. This substrate has been selected to match the nickel plating coefficient of thermal expansion (CTE), and minimize bi-metallic thermal effects that can be induced by a CTE mismatch between these materials. The surface deformations of the mirrors were simulated in a finite-element analysis (FEA) and the corresponding modified Zernike polynomials were determined and then put back into the optical model to determine the impact of the thermo-elastic, mounting, and gravity-induced deformations on the optical performances. The mirrors were diamond turned and post-polished to reach a surface roughness better than 1 nm rms. The wavefront of each mirror was individually measured before and after mounting. No deformation was observed. The RMS wavefront error remained below 35 nm. A field stop is located at the intermediate focal plane between the primary and secondary mirrors to minimize straylight. Two long-pass dichroïcs are used to separate the VNIR, the SWIR and the M/LWIR wavebands. The camera assembly is composed of the three detectors (VNIR, SWIR and M/LWIR) and of the second dichroic. It includes two stages of cooling. The first stage cools the SWIR array and environment to 180 K while the second stage cools down the M/LWIR array to 60 K. All the components are assembled on a carbon-fiber reinforced polymer. The optical layout and optical bench assembly is shown in Fig. 1.

One mirror assembly (mirror, bracket and panel) was subjected to a launch-level (GEV) vibration test. The variation of the wavefront after vibration remained within the measurement error (< 6 nm RMS).

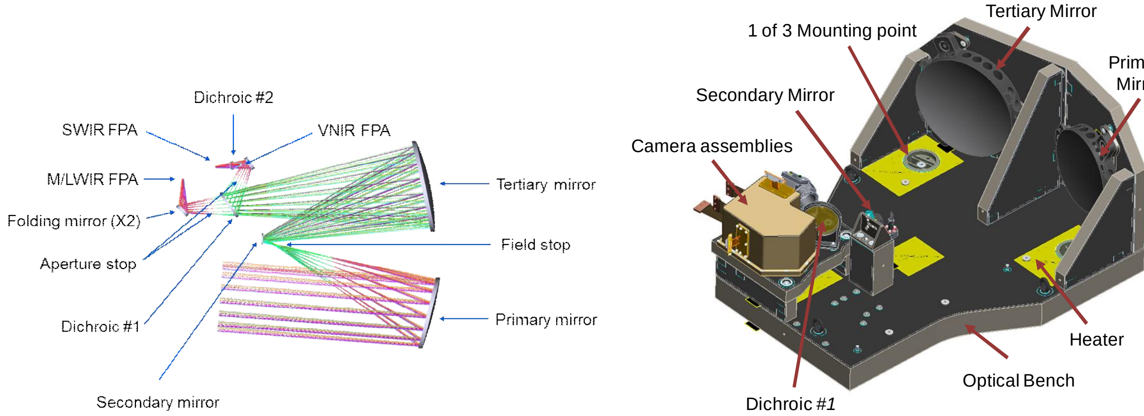

Fig. 1: TMA telescope optical layout (left panel) and 3-D view of the telescope breadboard (right panel)

IV. FILTER ASSEMBLIES

The multi-spectral images are acquired by using butcher-block bandpass filter arrays placed at 1 mm from the detectors. The SWIR and M/LWIR arrays were manufactured and tested in this STDP. The SWIR array is composed of four filters with individual filters having a clear aperture of 1.50 mm x 10.5 mm. The M/LWIR array has 10 filters having a clear aperture length of 10.5 mm and a width ranging from 0.58 to 1.00 mm and is shown in Fig. 2.

The bandpass filters have challenging requirements associated with the desired spectral shape for each filter, the out-of-band rejection, the straylight generation and the spectral stability and uniformity to be achieved. The difficulty is enhanced by the fact that the filters are placed close to the detector and are not only small but they also have strict dimensional tolerancing. They will also have to operate at cryogenic temperatures (60 K for the M/LWIR and 180 K for the SWIR). The optical bandpass filters and the dichroic filters have been identified for early development because of these challenges and because they are critical components of the MSCA itself. The goal is to achieve TRL 5 for these elements. They were designed, manufactured and tested at cryogenic temperature. Tests also included the standard adherence and abrasion tests on samples. Samples were also exposed to protons radiations (36 kRad). In general, the filters and dichroic beamsplitters survived all their environment tests without any apparent variation of their transmittance.

The SWIR filters bandpass measured at 293 K are compared to the designed curves at 293 K and 180 K in Fig. 2. The filter transmission is not expected to have a detectable performance variation between 293 K and 180K. The measured curves were slightly lower than the predicted ones but were still within requirements (see Fig. 3 left panel).

The first five M/LWIR theoretical transmission curves at 78K are shown in Fig. 3 right panel with two measured curves at 70K. These are also within requirements.

TRL5 was achieved for the filter assembly.

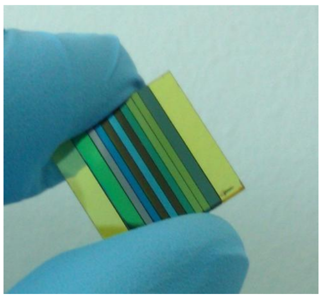

Fig. 2. M/LWIR Filter array made by Iridian Spectral Technologies

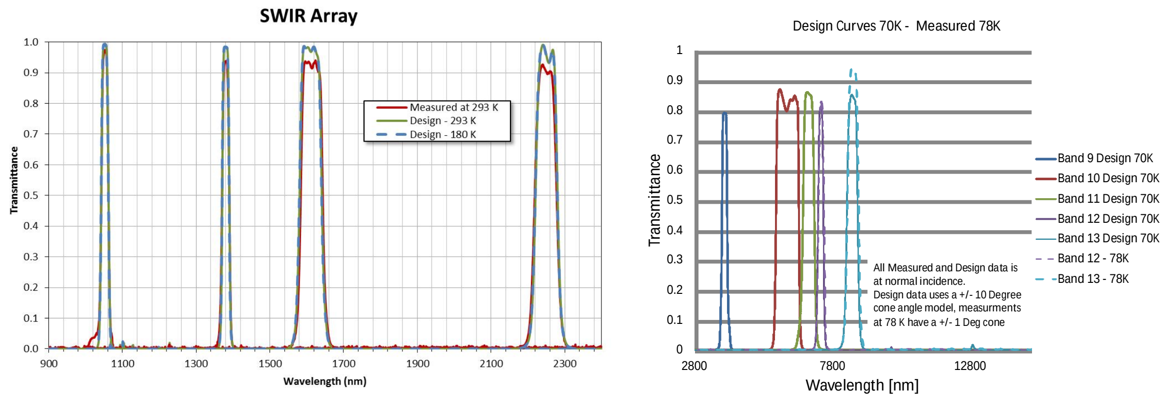

Fig. 3. Comparison of the SWIR (left panel) and the M/LWIR (right panel) measured transmission curves with the theoretical ones

V. OPTICAL TESTS

The Multi-Spectral Camera Assembly includes the thermal housing that enclose the dichroic beamsplitters, the bandpass filter arrays, the detector arrays and their proximity electronics, the thermal interface to the cryocooler and all the hardware to hold these components. In this STDP, the VNIR channel was simplified to a simple detector with no filter array mounted in front of it since only marginal TRL gain would have come out of manufacturing this element for a non-marginal cost.

Commercial detector arrays and proximity electronic boards were used, the emphasis of the project being on the assembly of the component and the overall functionality of the assembly itself rather than on detector development.

The MSCA and the Telescope Breadboard were joined to form a breadboard of the Multi-Spectral Imager (MSI). The MSI was subjected to tests in thermal vacuum that included thermal cycling to survival temperature and verification of imaging and radiometric performance at various thermal plateaus.

The imaging performances test setup referred to as the ground support equipment (GSE) is composed of a blackbody source illuminating a target located in the focal plane of a collimator that fills the entrance pupil of the PCW telescope. Available targets include US air force targets (USAF), slanted edges and pinholes. USAF targets images acquired in the VNIR, the SWIR and the M/LWIR are shown in the top panel of Fig. 4. The data are uncalibrated and uncorrected, we can thus distinguish the different spectral regions as horizontal stripes with slightly different intensities in the SWIR and M/LWIR images. The dark lines between the stripes are the shadows of the opaque adhesive between the filter stripes. The lowest bar frequency in those targets is 35 cycles/mm in the detector plane.

The MTF were measured by imaging horizontal and vertical slanted edges onto the detectors. The measured MTF in the VNIR channel acquired by placing a narrowband filter centred at 760 nm behind the slanted edge is shown in the bottom panel of Fig. 4. The GSD requirement of 0.5 to 1.5 km was flown down to a threshold MTF above 0.21 at 16.7 cycles/mm and a goal MTF above 0.27 at 50 cycles/mm. The measured MTF easily meets the threshold value while it is slightly under the goal value, as expected from the nominal design.

VI. STOP ANALYSIS

The mirrors in the PCW breadboard are mounted on a CFRP optical bench with an invar bracket. Invar was chosen to match the CFRP CTE but there is still a CTE mismatch remaining between the invar and the AlSi. The system is required to operate over a temperature ranging from 16.5 °C to 21.5 °C. The structural-thermal-optical performance analysis was conducted and showed that the surface deformation would exceed the surface tolerances. For this reason, thermal control was added to the mirrors to keep their temperature constant. The invar and CFRP having a small CTE, their contraction/dilatation over the required thermal range is negligible.

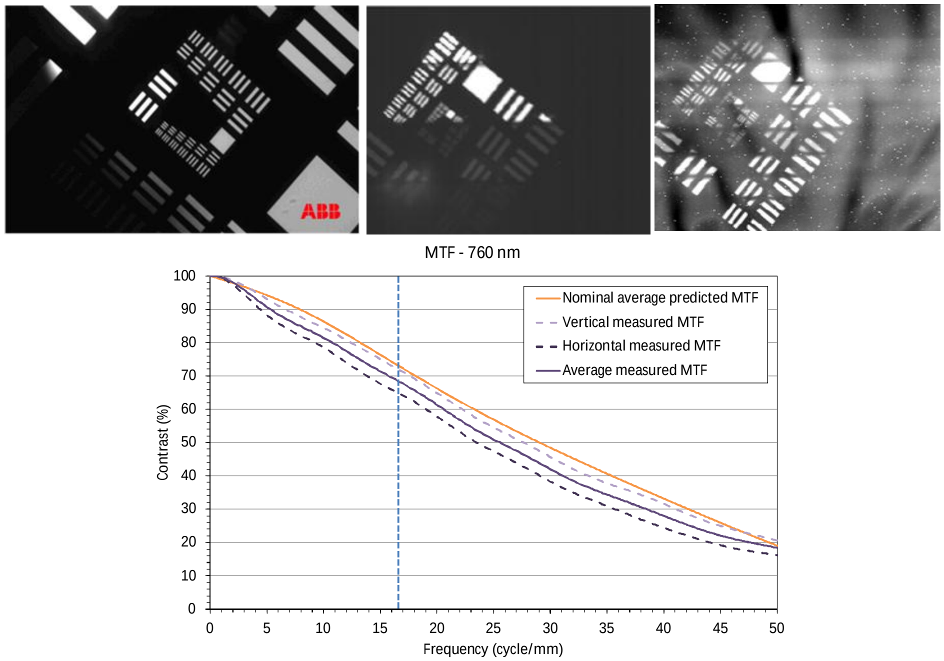

Fig. 4: VNIR, (top left) SWIR (top center) and M/LWIR (top right) images of a USAF resolution chart obtained with the Multi-Spectral Imager Breadboard. Raw uncalibrated and uncorrected data. The MTF measured at 760 nm in the VNIR channel is shown in the bottom panel.

This STOP analysis was validated with laboratory measurements for the tertiary mirror. The test setup is shown in the top panel of Fig. 5. The mirror is placed in a thermal-vacuum chamber (TVAC) to control its environment temperature. The Zygo interferometer is aligned with the tertiary mirror computer generated hologram (CGH) on an optical table having six degrees of liberty. These are then aligned with the tertiary mirror in the TVAC to minimize the aberrations on the Zygo interferometer. A reference measurement is taken at 22.5 °C and is subtracted from test measurements to extract the surface deformation induced by the temperature variations. This setup is sensitive to misalignments between the mirror and the Zygo/CGH that can be induced when changing the TVAC environment temperature. For this reason, the STOP analysis is validated by removing the power and astigmatism terms that are particularly sensitive to these misalignments. In a flight components test setup, the mirror movement in the TVAC would be tracked for compensation to avoid the removal of these terms. Note that the astigmatism induced by thermal deformations is expected to be small, hence we do not consider that its removal significantly impacts the surface irregularity assessment.

The simulated surface deformation induced by setting the environment temperature to 17.5 °C without thermal control on the mirror is shown in the bottom left panel of Fig. 5 while the measured value is shown in the bottom right panel. The aberration is dominated by primary trefoil induced by the mirror mounting points. The simulations predicted a RMS surface deformation of 0.100 wave while a deformation of 0.059 wave was measured, just below the surface irregularity tolerance of $\lambda/16$. The difference is believed to come from a conservative CTE value being used for the CFRP in the simulation compared to its real value. This resulted in a worst case scenario prediction for the surface deformation.

This demonstrates that the entirety of the surface irregularity tolerance budget is taken by thermal deformations with no thermal control. The next step was to turn the mirror thermal control ON. This resulted in a differential surface deformation of 0.004 wave, well below the $\lambda/16$ tolerance value. This shows that the thermal control is necessary and efficient at controlling the thermally induced surface deformations.

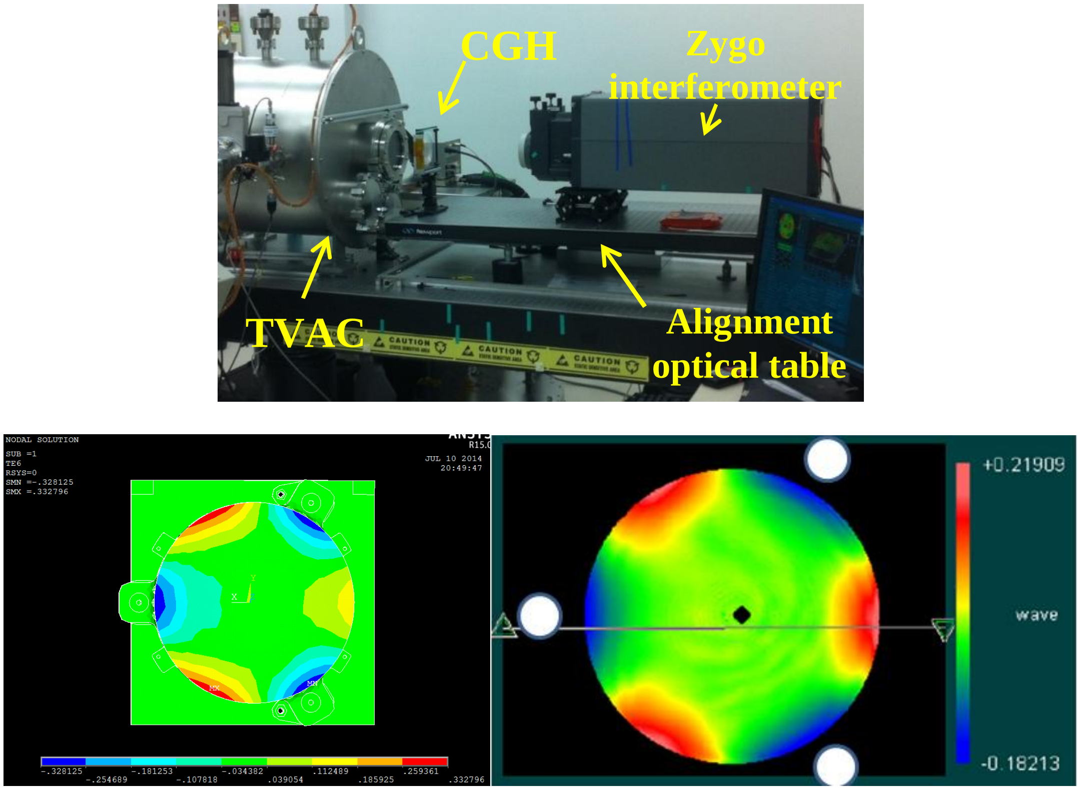

Fig. 5: The differential surface deformation for the tertiary mirror between a temperature of 22.5°C and 17°C simulated in the STOP analysis (bottom left) are compared to the laboratory measurement (bottom right). The power and astigmatism terms are removed from both results. The test setup is shown in the top panel.

VII. SUMMARY

The telescope assembly and the filter elements maturity was increased to TRL 5 through this STDP. The telescope was demonstrated to deliver the required MTF and it was demonstrated through STOP analysis and tests that thermal control over the mirrors is required to maintain the image quality in varying thermal conditions. The butcher-block filters were assembled for the SWIR and the M/LWR bands, tested at their operating temperature and mounted in front of their sensor for tests. Their requirements were met and TRL 5 was achieved.

The technology development activities were funded by the Space Technology Development Program of the Canadian Space Agency.

REFERENCES

[1] Trichtchenko, A. P., Garand, L., “Observing polar regions from space: advantages of a satellite system on a highly elliptical orbit versus a constellation of low Earth polar orbiters”, *Canadian Journal of Remote Sensing*, 38(1), 12-24, 2012.

[2] Garand, L., Kroupnik, G., “The Polar Communications and Weather (PCW) mission: a Canadian project to observe the Arctic region from a highly elliptical orbit”, *16th Conference on Satellite Meteorology and Oceanography*, 2009.

[3] Canadian Space Agency, “PCW Web Site at the Canadian Space Agency”, http://www.asc-csa.gc.ca/eng/satellites/pcw/

[4] Trichtchenko, A. P., Garand, L., “Canadian Polar Communication and Weather (PCW) satellite system: New capabilities for mapping Arctic snow and ice dynamics from Highly Elliptical Orbit”, *6th EARSel Workshop*, U. Of Bern, 2011.

[5] Garand, L., “The Polar Communications and Weather mission, a concrete solution for seamless observation of the Arctic”, Joint Center for Satellite Data Assimilation Seminar, 2010.

[6] Moreau, L., P. Dubois, F. Girard, F. Tanguay, J. Giroux. “Concept and Technology Development for the Multi-Spectral Imager of the Canadian Polar Communications and Weather Mission”, *Sensors, Systems, and Next-Generation Satellites XVI. Proceedings of the SPIE*, Volume 8533, 2012.